DALTON
FULL PAPER

Dynamic coordinative exchange in rhodium(I) complexes of chiral diphosphines bearing pendant pyridyl donor groups

Jonathan L. Bookham,*[a] Darren M. Smithies[a] and Mark Thornton Pett[b]

[a] *School of Applied and Molecular Sciences, University of Northumbria at Newcastle, Newcastle upon Tyne, UK NE1 8ST*
[b] *School of Chemistry, University of Leeds, Leeds, UK LS2 9JT*

Received 12th November 1999, Accepted 8th February 2000

meso-{$Ph_2PCH(Ph)CH(Ph)PPh_2$}, *meso*-{$Ph_2PCH(pyr)CH(pyr)PPh_2$}, *erythro*-{$Ph_2PCH(Ph)CH(pyr)PPh_2$}, *rac*-{$Ph_2PCH(pyr)CH(pyr)PPh_2$}, *threo*-{$Ph_2PCH(Ph)CH(pyr)PPh_2$}, and *threo*-{$Ph_2PCH(Ph)CH(pym)PPh_2$}, [pyr = 2-pyridyl, pym = 2-pyrimidyl] reacted with $[Rh(COD)Cl]_2$ (COD = 1,5-cyclooctadiene) to give cationic rhodium(I) complexes $[Rh(COD)\{L\}]^+$ (L = diphosphine ligand), which were isolated as their PF_6^- salts, **1**–**6** respectively. In **2** and in **3** the phosphine ligand adopts a P,P′,N-coordination mode whereas **1**, and **4**–**6** exhibit simple P,P′-coordination for the parent ligands and no evidence for N-coordination is observed. In solution **2** undergoes a fluxional process involving interchange of the coordinated and non-coordinated pyridyl environments. Variable temperature NMR studies revealed an enthalpy of activation ($\Delta H^{\ddagger}$) of 64.3 kJ mol^{-1} and an entropy of activation ($\Delta S^{\ddagger}$) of 0.005 kJ K^{-1} mol^{-1} for this process in *ortho*-dichlorobenzene solution. Complex **3** exhibits no similar fluxional behaviour. A single-crystal X-ray analysis of **2** revealed a nitrogen–rhodium distance of 2.369(3) Å for the coordinated pyridyl group, which is slightly longer than each of the phosphorus–rhodium distances [2.2868(7) Å and 2.3649(8) Å]. This suggests a relatively weak nitrogen–rhodium bonding interaction.

Introduction

The use of chiral bidentate phosphine ligands in metal-mediated asymmetric catalysis is now well-established and the published literature abounds with examples of their applications.[1] The variety of ligand types has expanded rapidly in recent years and there now exists a wide range of chiral bidentate ligands available to the synthetic chemist. In addition to the relatively simple C_2 symmetric diphosphine ligands such as '*chiraphos*' (2,3-bis(diphenylphosphino)butane)[2] and '*dipamp*' (1,2-bis[(*o*-methoxyphenyl)phenylphosphino]ethane),[3] a number of chiral heteroatomic donor ligands have been reported, examples being 1-(2-diphenylphosphino-1-naphthyl)isoquinoline, which has been shown to be an efficient agent in asymmetric hydroboration reactions,[4] and 2-[1-(1*S*,2*S*,5*R*)-(−)menthoxydiphenylphosphino]pyridine, which has been used successfully in the enantioselective hydroformylation of olefins.[5] Although a number of chiral mixed P,N donor ligands such as these have been developed for asymmetric syntheses recently,[6] very few are based on a simple C_2 symmetric structure[7a–c] and of these fewer still have the potential for simultaneous P- and N-coordination to a single metal centre.[7b,7c]

The presence of additional donor sites within a P_2-coordinated chiral diphosphine may affect dramatically the extent of asymmetric induction and catalytic efficiency during the course of a metal-mediated reaction. This could result either from additional coordination to the metal centre (whether static or dynamic) hence increasing the steric influence of the chiral ligand or, for example, from weak hydrogen-bonding interactions of the additional donor atoms with the reactant substrate itself.

To this end we have recently reported the synthesis and coordination behaviour of a range of chiral P_2N and P_2N_2 donor ligands, based on the $Ph_2PCH(Ar)CH(Ar')PPh_2$ structure, where Ar and Ar′ are various pyridyl, pyrimidyl and phenyl groups.[8] We have shown that all ligands readily adopt a simple P,P′-coordination mode in their octahedral Cr, Mo, and W tetracarbonyl complexes but additionally, in certain circumstances, N-coordination can also be achieved through carbonyl displacement to give *fac* P,P′,N-coordinated tricarbonyl derivatives. Additionally, the stereochemistry of the parent ligand is critical in determining: (i) the dominant solid- and solution-state chelate ring conformations in their P,P′-coordinated tetracarbonyl derivatives, (ii) the ability of the ligand to adopt a tridentate (P,P′,N)-coordination mode, and (iii) the propensity for inversion at an sp^3 hybridised backbone carbon atom in certain cases.[9]

In this paper we report investigations into the coordination chemistry of these chiral ambidentate diphosphine ligands in nominally square-planar environments and report synthetic, NMR, and selected X-ray diffraction studies of their 1,5-cyclooctadiene (COD) Rh(I) derivatives. In square planar complexes the chelate-ring conformations adopted in P,P′-coordinated complexes will not be influenced by steric repulsion from axial ligands and pyridyl coordination requires no associated axial ligand displacement. Hence these species serve as useful models for investigations into chiral ligand conformation and structure at square planar metal centres.

Results and discussion

Treatment of $[Rh(COD)Cl]_2$ with 2 molar equivalents of the appropriate diphosphine ligand (L) in the presence of ammonium hexafluorophosphate gave complexes of formula $[Rh(COD)(L)]^+PF_6^-$. Complexes **1** and **4**–**6** were isolated as air-stable red-orange crystalline solids and **2** and **3** were isolated as air-stable yellow crystalline solids. All complexes prepared dissolve readily in dichloromethane, but not in alcohols or ethers. Complexes **1**–**3** are also readily soluble in chloroform whereas **4**–**6** are essentially insoluble. Microanalytical data are shown in Table 1. All complexes reported here undergo decomposition rather than clean melting behaviour at elevated temperatures.

Fig. 1 shows the identity of the complexes reported herein.

DOI: 10.1039/a908984e

Table 1 Analytical data (%) for **1**–**6** with calculated values in parentheses

Compound	C	H	N
1[a]	59.3 (59.9)	4.8 (4.8)	0.0 (0.0)
2	60.0 (59.5)	4.6 (4.7)	1.6 (1.5)
3[b]	57.6 (58.0)	4.6 (4.7)	3.1 (3.1)
4	59.1 (59.5)	4.6 (4.7)	1.6 (1.5)
5	58.0 (58.1)	4.5 (4.6)	3.1 (3.1)
6	57.9 (58.1)	4.5 (4.6)	3.1 (3.1)

[a] Isolated as a 1:0.25 dichloromethane solvate to which these figures apply. [b] Isolated as a 1:0.25 methanol solvate to which these figures apply.

NMR studies

Selected NMR parameters for complexes **1**–**6** are given in Tables 2–4. The proton-decoupled ^{31}P NMR spectrum of **1** shows a simple doublet pattern (arising from scalar coupling to a single ^{103}Rh nucleus) for the two equivalent coordinated phosphorus atoms. The two chemically equivalent ligand backbone CH protons form the A part of an AA′XX′ spin system (X = ^{31}P).[10] The signal for these protons in the ^{1}H NMR spectrum therefore appears as a complex but characteristic multiplet at 4.24 ppm from which no individual coupling constant can be unambiguously identified. The *meso* stereochemistry of the parent phosphine ligand in **1** leads to two inequivalent environments for the four olefinic protons

Table 2 Selected proton NMR data for **1**–**6**[a]

Compound	$\delta(H^1)$[b]	$\delta(H^2)$[b]	$\delta(H^{3a-d})$[c]	$\delta(H^4)$[d]
1	4.24 [m]	4.24 [m]	4.82 (2H), 5.25 (2H)	—
2	4.56 [2.9, 5.2, 10.2]	4.80 [2.9, 10.5, 37.2]	3.82 (2H), 4.18 (2H)	9.66
3	4.43 [3.0, 5.8, 10.9]	4.50 [3.0, 9.9, 37.0]	3.85 (2H), 4.18 (2H)	9.65
4	4.34 [m]	4.34 [m]	4.94 (2H), 5.02 (2H)	7.82
5	4.52 [4.3, 7.3, 14.5]	4.69 [4.0, 6.4, 14.5]	4.35 (2H), 5.05 (2H)	7.96
6	4.63 [4.3, 8.0, 14.3]	4.76 [4.3, 6.1, 14.3]	4.35 (2H), 4.97 (1H), 5.15 (1H)	8.11

[a] Chemical shifts in ppm (±0.01 ppm) relative to internal TMS ($\delta = 0.0$), figures in square brackets are proton–proton and phosphorus–proton coupling constants in Hz (±0.2 Hz) listed arbitrarily in order of increasing magnitude, values of $^{3}J(H^1H^2)$ are underlined, m denotes a multiplet inappropriate for determination of couplings by inspection due to molecular symmetry. [b] Relative assignment of H^1 and H^2 is arbitrary and may be reversed. [c] Chemical shift values only, figures in parentheses are signal integrals. [d] Chemical shift values only.

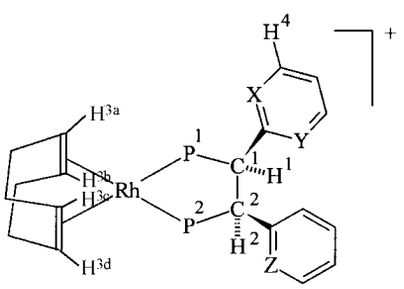

	X	Y	Z	*stereochemistry*
1	CH	CH	CH	*meso*

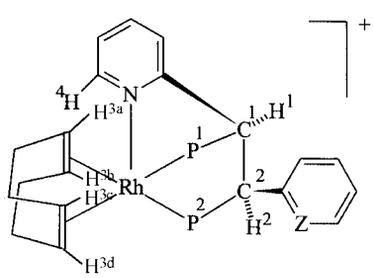

	Z	*stereochemistry*
2	N	*meso*
3	CH	*erythro*

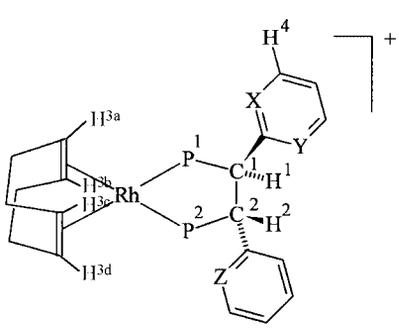

	X	Y	Z	*stereochemistry*
4	N	CH	N	*rac*
5	N	CH	CH	*threo*
6	N	N	CH	*threo*

Fig. 1 Schematic structures and partial NMR labelling system for the cations of **1**–**6**. Phenyl groups on the phosphorus atoms have been omitted for clarity. '*Stereochemistry*' refers to that of the parent ligand (before coordination). The relative assignment of H^{3a}–H^{3d} is arbitrary.

(H^{3a-3d}, see Fig. 1) of the COD ligand and the signals for these are at 4.82 and 5.25 ppm although their relative assignment is uncertain. The aromatic phenyl protons and the aliphatic CH_2 protons of the COD ligand give complex overlapping patterns centred around approximately 7.5 and 2.5 ppm respectively.

The effect of changing the phosphine ligand backbone substituents from phenyl to 2-pyridyl groups is profound and is manifested dramatically in the NMR spectra of **2**. The ^{31}P-$\{^1H\}$ NMR spectrum of **2** reveals two inequivalent P donor atoms with $J(PP) = 26.7$ Hz. Notable also are the smaller magnitudes of $^1J(^{103}Rh^{31}P)$ and the lower phosphorus-31 chemical shift values in **2** than in **1**. Additionally, at ambient temperature (295 K) in $CDCl_3$ all signals are perceptibly broadened. Essential features of the ^1H NMR spectrum of **2** are: (i) similar line-broadening to the ^{31}P-$\{^1H\}$ spectrum, (ii) inequivalent CH ligand backbone protons, (iii) lower olefinic COD proton chemical shifts than in **1** (approximately 4 ppm in **2** compared to 5 ppm in **1**), and (iv) a characteristic signal at 9.66 ppm. 2-D COSY experiments reveal that this signal is one from a spin system containing four inequivalent aromatic protons and is consistent only with one of the pyridyl groups. Its multiplicity reveals one large and two small (long-range) coupling constants and this together with its chemical shift then identifies it unambiguously as from H^4 on the single coordinated pyridyl ring (its high chemical shift is consistent with nitrogen-coordination as observed in related complexes we have previously reported).[8] All these features are consistent with the presence of N-coordination *via* ONE of the two pyridyl nitrogen atoms[11] but with an accompanying slow exchange of the two pyridyl environments as shown in Fig. 2 (see dynamic NMR studies later). Analogous features are observed in the ^{13}C spectrum. Diagnostic NMR parameters for **3** are essentially similar to **2** but all signals in all spectra are narrow and therefore suggest a fixed coordination of its single pyridyl group. In **2** and **3** $^3J(H^1H^2)$ is approximately 3 Hz and this corresponds to an H^1CCH^2 dihedral angle of approximately 60° based on a modified Karplus relationship.[12] This angle conforms with the respective *meso*- and *erythro*-stereochemistries of the parent ligands and is similar to that observed in analogous tricarbonyl derivatives reported previously.[8]

For **4**–**6** all spectra are consistent with a simple P,P′-coordination mode and no evidence for N-coordination is apparent even in **6** where the presence of a 2-pyrimidyl group provides two potential donor atoms. In these species $^3J(H^1H^2)$ (*ca*. 14.5 Hz where measurable) indicates an H^1CCH^2 dihedral angle of approximately 180°. This establishes the Ar and Ar′ groups in each case as occupying equatorial positions with respect to the chelate-ring, as we have also observed in their $M(CO)_4$ derivatives, rather than the alternative arrangement where both are axial. Together, therefore, these two studies reveal that, regardless of whether axial ligands are present or not, these ligands of *rac* or *threo* geometry adopt conformations with equatorial C-aryl substituents. This suggests that the dominant solution-state chelate-ring conformation is determined primarily from steric interactions within the ligand itself rather than from interactions between ligands. Additionally, these studies each show the reluctance of P,P′-coordinated ligands of *rac* or *threo* stereochemistry to undergo nitrogen-coordination, whereas the process is facile for their *meso* or *erythro* counterparts. In octahedral carbonyl complexes nitrogen coordination requires expulsion of a molecule of carbon monoxide and so the process is likely to be entropically favoured. In the present study however, N-coordination requires no attendant ligand displacement and the entropy contribution to the free energy of reaction should therefore be small. Despite this, N-coordination for ligands of *meso* or *erythro* occurs readily for the complexes reported herein, and the geometry and coordination number of the metal and its electron count all change as a result.

Table 3 Phosphorus-31 NMR data for **1**–**6**[a]

Compound	$\delta(^{31}P^1)$[b]	$\delta(^{31}P^2)$[b]	$J(P^1P^2)$[c]
1	56.2 [144]	56.2 [144]	[d]
2	50.1 [117]	52.6 [109]	26.7
3	49.9 [108]	53.1 [120]	26.5
4	58.2 [149]	58.2 [149]	[d]
5	58.3 [149]	59.1 [144]	39.0
6	57.3 [149]	59.4 [144]	39.0

[a] Chemical shifts in ppm (±0.2 ppm) relative to external 85% H_3PO_4 ($\delta = 0.0$), figures in square brackets are values of $^1J(^{103}Rh^{31}P)$ (±1 Hz). [b] Relative assignment of P^1 and P^2 is arbitrary and may be reversed. [c] In Hz (±0.2 Hz). [d] Not determined by inspection due to molecular symmetry.

Table 4 Selected carbon-13 NMR data for **1**–**6**[a]

Compound	$\delta(^{13}C^1)$[b]	$\delta(^{13}C^2)$[b]	$\delta(^{13}C^{3a-d})$[c]
1	53.0 [m]	53.0 [m]	101.2, 102.1
2	48.9 [21.1, 21.1]	55.4 [11.0, 26.0]	82.6, 85.4
3	47.1 [22.5, 22.5]	56.7 [12.8, 23.0]	83.3, 87.1
4	49.4 [2.8, *49.4*]	49.4 [2.8, *49.4*]	100.5, 106.6
5	47.9 [2.5, 21.5, 23.5]	49.4 [2.0, 24.2, 24.2]	100.5, 106.7
6	48.5 [2.8, 21.1, 26.6]	50.0 [2.2, 23.8, 23.8]	100.6, 106.8

[a] Chemical shifts in ppm (±0.1 ppm) relative to internal TMS ($\delta = 0.0$), figures in square brackets are rhodium–carbon (underlined) and phosphorus–carbon coupling constants in Hz (±0.2 Hz) listed in order of increasing magnitude, m denotes a multiplet inappropriate for determination of couplings by inspection due to molecular symmetry, figures in italics are values of $|^1J(^{31}P^{13}C) + {}^2J(^{31}P^{13}C)|$ where individual components cannot be determined due to molecular symmetry. [b] Relative assignment of C^1 and C^2 is arbitrary and may be reversed. [c] Two distinct chemical shift regions observable in each case.

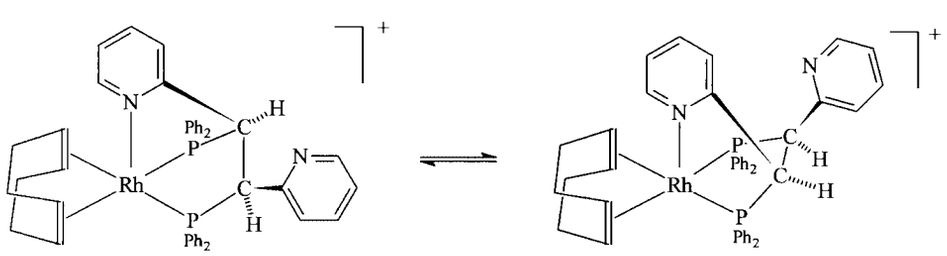

Fig. 2 Representation of the fluxional behaviour available to compound **2**.

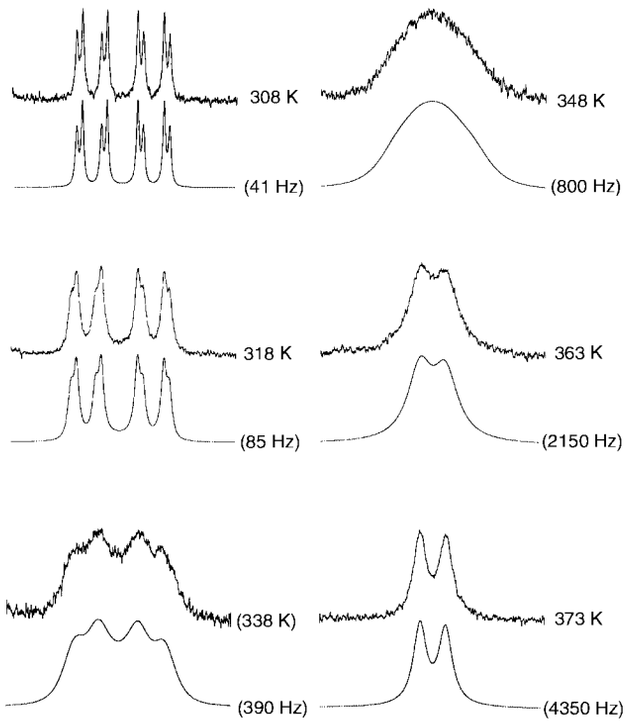

Fig. 3 Upper traces: portions of the $^{31}P-\{^{1}H\}$ NMR spectra of **2** at selected temperatures (solvent = *ortho*-dichlorobenzene). Lower traces: computer simulated spectra using *gNMR*—calculated exchange rates ($1/\tau$) are shown in parentheses.

Dynamic NMR studies

$^{31}P-\{^{1}H\}$ spectra of **2** in *ortho*-dichlorobenzene at selected temperatures and corresponding computer simulated spectra (fitted to a ABX spin system where A, B = ^{31}P, X = ^{103}Rh) based on an interchange of the two phosphorus environments are shown in Fig. 3. A standard Eyring plot [13] of $\ln(k/T)$ against $1/T$ (k = rate calculated from computational simulation,[14] T = absolute temperature) gives an enthalpy of activation ($\Delta H^{\ddagger}$) of 64.3 (±2.6) kJ mol^{-1} and an entropy of activation ($\Delta S^{\ddagger}$) of 5.0 (±7.8) J K^{-1} mol^{-1}, (figures in parentheses refer to the 95% confidence limits after linear regression).† This latter value suggests that the exchange process does not involve an additional participating ligand in this solvent. In the potentially more strongly coordinating solvent d_6-DMSO the patterns of spectra are similar but the onset of decomposition at 60° precludes studies across the same temperature range as that available for solutions in *ortho*-dichlorobenzene.

Single-crystal X-ray analysis of compound 2

Crystals of compound **2** suitable for X-ray diffraction analysis were obtained as a 1 : 1 dichloromethane solvate by diffusion of methanol into a solution of **2** in dichloromethane.‡ An ORTEP-type [15] drawing of the structure of the cation is shown in Fig. 4. Crystallographic data and selected interatomic distances and angles between interatomic vectors are shown in Tables 5 and 6 respectively.

The immediate environment around the rhodium atom is completely asymmetric and is most conveniently described as seven-coordinate with bonds to the four olefinic COD carbons and the P,P′,N-coordinated phosphine ligand. The Rh(1)–P(1) and Rh(1)–P(2) bond lengths are 2.3649(8) and 2.2868(7) Å and are close to those observed in a range of COD rhodium(I) complexes containing di- and triphosphine ligands (typically, close to 2.3 Å).[16] Surprisingly, the Rh(1)–N(133) distance of 2.369(3) Å is greater than either Rh–P distance within the molecule. Published structures suitable for direct comparison are few, but the bidentate phosphino/pyridine ligands 1-diphenylphosphino-1′-(2-pyridyl)ferrocene and 2-pyridylmethyl(methyl)phenylphosphine coordinate to rhodium with Rh–P distances of 2.326 and 2.255 Å respectively and Rh–N distances of 2.136 and 2.116 Å respectively in their analogous COD derivatives.[17] Similarly in the *fac*-P,P′,N-coordinated octahedral $Mo(CO)_3$ analogue of **2** [18] the corresponding Rh–N distance is approximately 0.2 Å shorter than the Rh–P distances and entirely consistent with a strong bonding interaction. The Rh(1)–N(133) bonding interaction in **2** therefore appears to be

† Least squares linear regression on 8 observations (6 shown in Fig. 3) yielded a slope [$-\Delta H^{\ddagger}/R$] of −7731.6 (±315) and an intercept [$= 23.76 + \Delta S^{\ddagger}/R$] of 23.078 (±0.95) with an adjusted R^2 value of 0.998.

‡ Compound **2** was recrystallised from chloroform–methanol to give an analytically pure sample (C,H,N analyses are in Table 1) but crystals better suited to X-ray diffraction studies were subsequently obtained by crystallisation from a solution in dichloromethane–methanol.

Table 5 Crystal data and structure refinement for compound **2**

Empirical formula	$C_{45}H_{44}Cl_2F_6N_2P_3Rh$
Formula weight	993.54
Temperature/K	150(2)
Wavelength/Å	0.71073 [Mo-Kα]
Crystal system	Monoclinic
Space group	$P2_1/c$
a/Å	11.0292(2)
b/Å	14.1653(3)
c/Å	28.2016(5)
β/°	101.0150(10)
Volume/Å^3	4324.82(14)
Z	4
Density (calculated)/Mg m^{-3}	1.526
Absorption coefficient/mm^{-1}	0.691
F(000)	2024
Crystal size/mm	0.63 × 0.36 × 0.30
Data collection range	$2.37 \le \theta \le 26.00°$
Index ranges	$-13 \le h \le 13$, $-17 \le k \le 17$, $-34 \le l \le 34$
Reflections collected	30701
Independent reflections	8465 [R(int) = 0.0515]
Absorption correction	Multi-scan
Max. and min. transmission	0.8196 and 0.6701
Refinement method	Full-matrix least-squares on F^2
Data/restraints/parameters	8465/20/549
Goodness-of-fit on F^2	1.063
Final R indices [$I > 2\sigma(I)$]	$R_1 = 0.0433$, $wR_2 = 0.1143$
R indices (all data)	$R_1 = 0.0475$, $wR_2 = 0.1178$
Largest diff. peak and hole/e Å^{-3}	1.038 and −0.957
Extinction coefficient	0.0027(5)

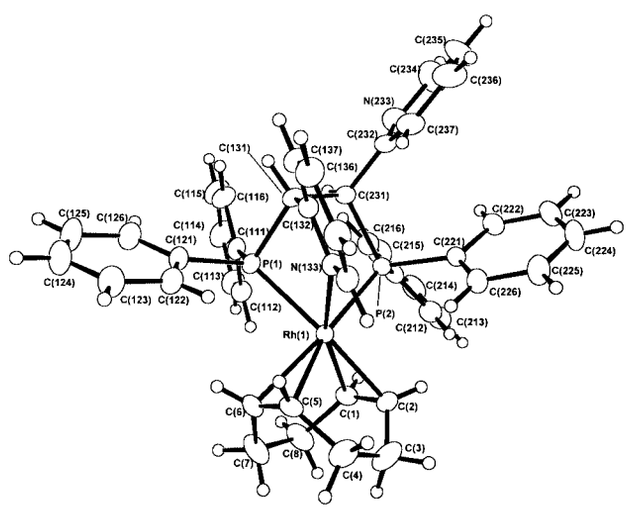

Fig. 4 An ORTEP-type [15] drawing of the cation of compound **2**. Ellipsoids are shown at the 40% probability level, hydrogens have been drawn as circles with an arbitrary small radius.

Table 6 Selected interatomic distances (Å) and interbond angles (°) for compound **2** with e.s.d.s in parentheses

Rh–C(1)	2.110(3)	Rh–C(2)	2.147(3)
Rh–C(5)	2.257(3)	Rh–P(2)	2.2868(7)
Rh–C(6)	2.302(3)	Rh–P(1)	2.3649(8)
Rh–N(133)	2.369(3)	C(1)–C(2)	1.410(5)
C(1)–C(8)	1.525(5)	C(2)–C(3)	1.518(5)
C(3)–C(4)	1.467(6)	C(4)–C(5)	1.510(5)
C(5)–C(6)	1.365(5)	C(6)–C(7)	1.510(5)
C(7)–C(8)	1.470(5)		
P(2)–Rh–P(1)	83.19(3)	P(2)–Rh–N(133)	81.73(6)
P(1)–Rh–N(133)	75.38(6)		

relatively weak. In contrast, no obvious weak coordination of an additional third donor atom is apparent in P,P′,P″-coordinated rhodium/COD analogues of which a small number have been reported.[19] The relatively weak coordination in **2** may therefore be explained by the strain induced when the tridentate coordination mode is adopted, however the P(1)–Rh(1)–P(2), P(1)–Rh(1)–N(133) and P(2)–Rh(1)–N(133) interbond angles of 83.19(3), 75.38(6), and 81.73(6)° respectively bear a close resemblance to those in its *fac*-P,P′,N′-coordinated $Mo(CO)_3$ derivative (81.00, 73.27 and 79.17° respectively) where a strong N-coordination is observed.[18] Alternatively, this weak coordination may simply be explained by a reluctance of the rhodium to increase its formal electron count and coordination number and thus its electron density, especially *via* coordination of a relatively poor π-acceptor such as a nitrogen atom.

Apparent also, is a clear differentiation in the Rh–C distances for the COD ligand. The Rh–C(1) and Rh–C(2) distances of 2.110(3) and 2.147(3) Å are somewhat shorter than the Rh–C(5) and Rh–C(6) distances [2.257(3) and 2.302(3) Å] and suggest a slightly weaker coordination of the C(5)/C(6) double bond to the rhodium atom relative to that of C(1)/C(2). This may occur simply to compensate for the increase in electron density caused by coordination of the pyridyl nitrogen. However, it should be noted that quite wide variations (2.0–2.4 Å) are common among Rh–C distances in Rh(I) COD complexes containing phosphine ligands[16–18] so this differentiation may be due to more general bulk effects such as crystal-packing forces.

Experimental

Solvents were dried and deareated by standard procedures before use and all manipulations were performed under an atmosphere of dry N_2. Phosphine ligands were prepared by previously published methods.[8] Rhodium complexes were prepared from $[Rh(COD)Cl]_2$[20] using a modification of the method of Shrock and Osborn,[21] a typical procedure is as follows:

[Rh(COD){*meso*-($Ph_2PCH(Ph)CH(Ph)PPh_2$)}]$^+PF_6^-$ (1)

meso-{$Ph_2PCH(Ph)CH(Ph)PPh_2$} (1.1 g, 20 mmol) and $[Rh(COD)Cl]_2$ (0.49 g, 10 mmol) in dichloromethane (25 cm^3) together with a solution of ammonium hexafluorophosphate (0.5 g, 30 mmol, excess) in distilled water (25 cm^3) were stirred under an atmosphere of nitrogen at room temperature for 1 h. The mixture was transferred to a separating funnel, the aqueous layer was removed and the red-orange dichloromethane layer was washed once with distilled water (20 cm^3) and then dried over anhydrous sodium sulfate. After filtration, methanol (20 cm^3) and diethyl ether (10 cm^3) were added to the solution and the mixture was refrigerated until crystallisation appeared complete. The crude product (1.4 g, 73%) was recrystallised from dichloromethane–methanol to give a red-orange crystalline solid.

Compounds **2**–**5** were prepared from the appropriate parent phosphine using a similar method to that described above. Yields were typically 70–80% before recrystallisation from either chloroform–methanol (**2**, **3**) or dichloromethane–methanol (**4**–**6**) which in all cases yielded analytically pure crystalline solids (see Table 1).‡

NMR spectra were obtained using a JEOL EX270 NMR spectrometer from solutions contained in 5 mm outer diameter tubes.

Crystallography

Data were collected on a Nonius KappaCCD, Mo-Kα radiation, 150 K and corrected for absortion semiempirically.[22] $\mu = 0.691$ mm^{-1}, $R_{int} = 0.0515$. The structure was solved by direct methods (SHELXS97)[23] and refined by full-matrix least squares (SHELXL-97)[24] on F^2 of all unique data to $R_1 = 0.0433$ $[I > 2.0\sigma(I)]$, $wR_2 = 0.1178$ (all data), $S = 1.063$. Non-hydrogen atoms were refined with anisotropic displacement parameters. Restraints were applied to the aromatic rings so they remained flat. Hydrogen atoms were constrained to idealised positions using a riding model. Full details of crystal data, data collection and structure refinement are given in Table 5.

CCDC reference number 186/1847.

See http://www.rsc.org/suppdata/dt/a9/a908984e/ for crystallographic files in .cif format.

References

1 See for example: R. Noyori, *Asymmetric Catalysis in Organic Synthesis*, Wiley, Chichester, 1994; H. B. Kagan and M. Sasaki, in *The Chemistry of Organophosphorus Compounds*, ed. F. R. Hartley, Wiley, Chichester, 1990, vol. 1, p. 173.
2 M. D. Fryzuk and B. Bosnich, *J. Am. Chem. Soc.*, 1977, **99**, 6262.
3 B. D. Vineyard, W. S. Knowles, M. J. Sabacky, G. L. Backman and O. J. Weinkauff, *J. Am. Chem. Soc.*, 1977, **99**, 5946.
4 N. W. Alcock, J. M. Brown and D. I Hulmes, *Tetrahedron: Asymmetry*, 1993, **4**, 742; J. M. Brown, D. I. Hulmes and T. P Layzell, *J. Chem. Soc., Chem. Commun.*, 1993, 1673.
5 C. G. Arena, F. Nicolo, D. Drommi, G. Bruno and J. N. Faraone, *J. Chem. Soc., Chem. Commun.*, 1994, 2251.
6 See for example: G. R. Newkome, *Chem. Rev.*, 1993, **93**, 2067; A. Albinati, F. Lianza, H. Berger, P. S. Pregosin, H. Rüegger and R. W. Kunz, *Inorg. Chem.*, 1993, **32**, 478; G. S. He, S. K. Lok, J. J. Vittal, K. F. Mok and P. H. Leung, *Organometallics*, 1998, **17**, 3931; G. Francio, C. G. Arena, M. Panzalorto, G. Bruno and F. Faraone, *Inorg. Chim. Acta*, 1998, **277**, 119.
7 (*a*) W. H. Hu, C. C. Pai, C. C. Chen, G. P. Xue and A. S. C. Chan, *Tetrahedron: Asymmetry*, 1998, **9**, 3241; (*b*) Q. Jiang, D. Van Plew, S. Murtaza and X. Zhang, *Tetrahedron Lett.*, 1996, **37**, 797; (*c*) P. H. M. Budzelaar, J. H. G. Frijns and A. G. Orpen, *Organometallics*, 1990, **9**, 1222.
8 J. L. Bookham and D. S. Smithies, *J. Organomet. Chem.*, 1999, **577**, 305.
9 J. L. Bookham, *Inorg. Chem. Commun.*, 1998, **1**, 309.
10 J. W. Emsley, J. Feeney and L. H. Sutcliffe, *High Resolution NMR Spectroscopy*, Pergamon, Oxford, 1965, vol. 1.
11 J. G. Verkade and L. D. Quin, in *Phosphorus-31 NMR spectroscopy in Stereochemical Analysis*, VCH, Deerfield Beach, FL, 1987.
12 M. Karplus, *J. Am. Chem. Soc.*, 1963, **85**, 2870; C. J. Hawkins and J. A. Palmer, *Coord. Chem. Rev.*, 1982, **44**, 1.
13 See for example: H. Günther, in *NMR Spetcroscopy*, 2nd edn., Wiley, Chichester, 1994.
14 P. H. M. Budzelaar, *gNMR V4.0*, Cherwell Scientific, Oxford, 1996.
15 P. McArdle, *J. Appl. Crystallogr.*, 1995, **28**, 65.
16 R. G. Ball and N. C. Payne, *Inorg. Chem.*, 1977, **16**, 1187; E. Cesarotti, A. Chiesa, G. Ciani and A. Sironi, *J. Organomet. Chem.*, 1983, **79**, 251; M. J. Burk, J. E. Feaster and R. L. Harlow, *Organometallics*, 1990, **9**, 2653; A. Borner, A. Kless, R. Kempe, D. Heller, J. Holz and W. Baumann, *Chem. Ber.*, 1995, **128**, 767.
17 T. Yoshida, K. Tani, T. Yamagat, Y. Tatsuno and T. Saito, *J. Chem. Soc., Chem. Commun.*, 1990, 292; H. Yang, N. Lugan and R. Mathieu, *Organometallics*, 1997, **16**, 2089.
18 J. L. Bookham, D. M. Smithies and M. Thornton-Pett, unpublished work.

19 J. Scherer, G. Huttner, O. Walter, B. C. Janssen and K. Zsolnai, *Chem. Ber.*, 1996, **129**, 1603.
20 G. Giordano and R. H. Crabtree, in *Inorganic Syntheses: Reagents for Transition Metal Complex and Organometallic Syntheses*, ed. R. J. Angelici, Wiley, Chichester, 1990, **28**, 88.
21 R. R. Shrock and J. A. Osborn, *J. Am. Chem. Soc.*, 1971, **93**, 2397.
22 R. H. Blessing, *Acta Crystallogr.*, *Sect. A*, 1995, **51**, 33.
23 G. M. Sheldrick, *Acta Crystallogr.*, *Sect. A*, 1990, **46**, 467.
24 G. M. Sheldrick, SHELXL-97, Program for the refinement of crystal structures, University of Göttingen, 1997.

Paper a908984e